J Mater Sci (2011) 46:3415–3423
DOI 10.1007/s10853-010-5230-9

# Phase, microstructural characterization and dielectric properties of Ca-substituted $Sr_5Nb_4TiO_{17}$ ceramics

**A. Manan · Y. Iqbal · I. Qazi**

Received: 22 September 2010 / Accepted: 29 December 2010 / Published online: 8 January 2011


**Abstract** The effect of Ca substitution for Sr on the phase, microstructure and microwave dielectric properties of the $Sr_{5-x}Ca_xNb_4TiO_{17}$ composition series was investigated using X-ray diffraction (XRD), scanning electron microscopy (SEM), an LCR meter, and vector network analyzer. Below 1450 °C, $Sr_{5-x}Ca_xNb_4TiO_{17}$ ($x = 1$, 2, 3, or 4) compositions formed single-phase $Sr_4CaNb_4TiO_{17}$, $Sr_3Ca_2Nb_4TiO_{17}$, $Sr_2Ca_3Nb_4TiO_{17}$, and $SrCa_4Nb_4TiO_{17}$ ceramics, respectively. At $x = 0$ and 5, $Sr_5Nb_4TiO_{17}$ and $Ca_5Nb_4TiO_{17}$ formed, but along with $Sr_2Nb_2O_7$ (at $x = 0$) and $CaNbO_3$ and $CaNb_2O_6$ (at $x = 5$) secondary phases. Above 1450 °C, all the compositions formed two-phase ceramics. At low frequencies, a phase transition was observed in the composition $Sr_5Nb_4TiO_{17}$. The substitution of Ca for Sr enabled processing of highly dense $Sr_2Ca_3Nb_4TiO_{17}$, with $\varepsilon_r \sim 53.4$, $\tau_f \sim -6.5$ ppm/°C and $Q_u \times f_o \sim 1166$ GHz. Further investigations are required to improve the quality factor of these ceramics for possible microwave applications.

A. Manan · Y. Iqbal (✉)
Materials Research Laboratory, Institute of Physics and Electronics, University of Peshawar, Peshawar 25120, Pakistan
e-mail: dryaseeniqbal@yahoo.co.uk

A. Manan
e-mail: abdul_manan_sher@yahoo.com

A. Manan
Department of Engineering Materials, University of Sheffield, Sir Robert Hadfield Building, Sheffield S1 3JD, UK

I. Qazi
Department of Materials Science and Engineering, Institute of Space Technology, P.O. Box 2750, Islamabad 44000, Pakistan
e-mail: Ibrahim.qazi@ist.edu.pk

## Introduction

Ceramic dielectric resonators (DRs) used at microwave frequencies have been utilized for the last few decades in mobile telecommunications devices. The three key parameters needed for a material to be used as a microwave DR are (a) a high dielectric constant (especially for handsets) to reduce the size of the microwave component, (b) low dielectric loss (implying a high quality factor, $Q_u$, where $Q_u = 1/\tan\delta$) for fine tuning and (c) a near-zero temperature coefficient of resonant frequency to ensure temperature stability of the microwave component. Only a few materials meet this industrial requirement. Examples include $Ba(Zn_{1/3}Ta_{2/3})O_3$, $BaTi_4O_9$, $Ba_2Ti_9O_{20}$, $(Zr,Sn)TiO_4$, and $Ba_{6-3x}Re_{8+2x}Ti_{18}O_{54}$ (Re = Nd, Sm, La), all of which are used at microwave frequencies in various filters and oscillators in telecommunication devices [1]. Generally, a high dielectric constant material exhibits high loss and vice versa [2, 3]; therefore, it is difficult to have materials exhibiting all the above mentioned three properties simultaneously and there is a constant demand for new materials with better dielectric properties.

A number of dielectric ceramics belonging to the $A_nB_nO_{3n+2}$ series are known to exhibit good microwave properties. For example, $(CaLa_4)Ti_5O_{17}$ with $n = 5$ and $CaLa_8Ti_9O_{31}$ with $n = 4.5$ (i.e., $(Ca_{0.5}La_4)(Ti_{4.5})O_{15.5}$) are layered perovskites, with dielectric constants $\varepsilon_r = 55.2$ and 54.9, quality factors $Q_u \times f_o = 17359$ GHz (at 3.67 GHz) and 19345 GHz (at 3.65 GHz), and temperature coefficients of resonant frequency $\tau_f = -20$ and $-6$ ppm/°C, respectively [2]. Substitution of 1 wt% of Ca by Zn in $CaLa_4Ti_5O_{17}$ has been reported to give $\varepsilon_r = 57.6$, $Q_u \times f_o = 17100$ GHz and $\tau_f \sim 4.9$ ppm/°C [3]. Similarly, the addition of 0.5 wt% CuO as a sintering aid to $Ca_{0.99}Zn_{0.01}La_4TiO_{17}$ resulted in $\varepsilon_r = 57$, $Q_u \times f_o = 15000$ GHz and $\tau_f \sim -8.16$ ppm/°C at

1450 °C in comparison with 1500 °C for pure $Ca_{0.99}Zn_{0.01}La_4Ti_4O_{17}$ [4]. The substitution of 1 wt% of Ca by Mg in $CaLa_4Ti_5O_{17}$ gave $\varepsilon_r = 56.3$, $Q_u \times f_o = 12300$ GHz and $\tau_f \sim -9.6$ ppm/°C [5]. Anjana et al. [6] reported that $Ca_5Nb_4TiO_{17}$ and $Ca_3Mg_2Nb_4TiO_{17}$ have $\varepsilon_r = 45$, $Q_u \times f_o = 17600$ GHz and $\tau_f \sim -113$ ppm/°C and $\varepsilon_r = 37.5$, $Q_u \times f_o = 22500$ GHz and $\tau_f \sim -4.3$ ppm/°C, respectively. More recently, Joseph et al. [7] reported $Ca_5Nb_4TiO_{17}$ and $Ca_5Ta_5TiO_{17}$ to have $\varepsilon_r = 44.9$, $Q_u \times f_o = 17600$ GHz and $\tau_f \sim -112.9$ ppm/°C and $\varepsilon_r = 40.1$, $Q_u \times f_o = 16450$ GHz and $\tau_f \sim -53.6$ ppm/°C, respectively.

Slobodyanik et al. [8] synthesized $Ca_{5-x}Sr_xTiNb_4O_{17}$ with $0 \leq x \leq 5$ via co-precipitation of hydroxocarbonates, observed the beginning of $Sr_5TiNb_4O_{17}$ formation at temperatures above 1300 °C, and noted the requirement of temperatures well above 1400 °C for the formation of single-phase $Sr_5TiNb_4O_{17}$ ceramics. They did not measure the dielectric properties. Iqbal and Reaney [9] reported the dielectric constant $\varepsilon_r \sim 57$ (at 10 kHz), $Q_u \times f_o \sim 1070$ MHz and $TC\varepsilon \sim -0.0007$ ppm/°C for $Sr_5Nb_4TiO_{17}$ with no Ca. The crystal structure of $Sr_5Nb_4TiO_{17}$ is reported to be orthorhombic with space group *Pnnm* and lattice parameters $a = 5.6614$ Å, $b = 32.515$ Å, $c = 3.9525$ Å, and $Z = 2$ [10].

Keeping in view the high loss of $Sr_5Nb_4TiO_{17}$, the effect of Ca substitution on the phase, microstructure and dielectric properties of $Sr_5Nb_4TiO_{17}$ has been investigated as an attempt to improve $Q_u \times f_o$ for possible microwave applications.

## Experimental procedure

$Sr_{5-x}Ca_xNb_4TiO_{17}$ compositions ($x = 0$, 1, 2, 3, 4, and 5) were prepared via a mixed-oxide solid-state route. Laboratory reagent grade $SrCO_3$, $CaCO_3$ (Fisher Scientific, > 99%), $Nb_2O_5$ (BDH Chemicals Ltd., > 99.9%) and $TiO_2$ (Aldrich Chemicals, 99 + %), powders were weighed according to the stoichiometric ratios. The mixtures were milled for 60 h in disposable polyethylene mill jars with cylindrical Y-toughened $ZrO_2$ balls as grinding media and 2-praponol as lubricant using a conventional horizontal ball mill. The slurry was dried in an oven at ~95 °C overnight and the resulting powder samples were sieved to dissociate agglomerates (if any). Thermogravometric (TG) analysis and differential thermal analysis (DTA) were performed from room temperature to 1200 °C at 5 °C/min (for $x \leq 1$) and 10 °C/min (for $2 \geq x \geq 5$) for as-mixed $Sr_{5-x}Ca_xNb_4TiO_{17}$ compositions to determine the weight loss and phase transformation temperatures. The $Sr_5Nb_4TiO_{17}$ composition was calcined at 990 °C for 2 h. The other batches were calcined at 1350 °C for 2 h. Heating/cooling rates were 10 °C/min. The calcined powders were re-milled for 30 min and dried before uniaxial pressing into 13 mm diameter pellets at 140 MPa in a stainless steel die. The pellets were sintered in air at 1400–1550 °C for 2 h at heating/cooling rate of 10 °C/min. Sintered pellets were pulverized in a pestle and mortar system and ground into fine powders for XRD. A STOE PSD X-ray diffractometer with $CuK\alpha_1$ radiation ($\lambda = 1.540598$ Å) was used for phase analysis and measurement of lattice parameters. The sintered samples were finely polished and thermally etched at temperatures 10% less than the corresponding sintering temperatures and gold coated for microstructural analysis. Microstructural characterization was performed using a JEOL 6400 SEM operating at 20 kV, equipped with an energy dispersive X-ray spectroscopy (EDS) detector (Link, Oxford Instruments). The apparent density of the sintered pellets was measured using the Archimedes method. The theoretical densities of the compositions were calculated by using Eq. (1);

$$R_{th} = (ZM)/(A_g V) \quad (1)$$

where $Z$ is the number of formula units per unit cell, $M$ is the molecular weight, $V$ is the volume of the unit cell and $A_g$ is the Avogadro number ($6.022 \times 10^{23}$ atoms/mole).

The faces of the sintered pellets were coated with gold paste and heated to 800 °C for 2 h at 10 °C/min. The dielectric constant was measured from 1 kHz to 1 MHz at temperatures ranging from 20 to 800 °C using a HP 4284A LCR meter. For loss tangent measurements, the sintered pellets were mounted on a low-loss quartz single crystal at the centre of a 20 mm diameter cavity made of brass to avoid conduction loss. The microwave energy was coupled to the test piece using two ports. Measurements were taken in transmission mode using a network analyzer (R3767CH, Advantest). The average temperature coefficient of resonant frequency, $\tau_f$, between 20 and 70 °C was calculated using Eq. (2);

$$\tau_f = (f_2 - f_1)/(f_1 \Delta T) \quad (2)$$

where $f_1$ is the resonant frequency at 20 °C and $f_2$ at 70 °C, and $\Delta T$ is the difference between the initial (~20 °C) and final temperature (~70 °C) of measurement.

## Results and discussion

### TG/DTA analysis

TG/DTA curves from as mix-milled $3SrCO_3$:$2CaCO_3$:$2Nb_2O_5$:$1TiO_2$ powders are shown in Fig. 1. A careful examination of the TGA curve indicated the beginning of mass loss at 650 °C, which continued till 750 °C, due to

the decomposition of $CaCO_3$ [11]. Another downward slope was observed just after 750 °C which continued until 902 °C, probably due to the decomposition of $SrCO_3$ [12]. The observed increase in the decomposition temperature of $SrCO_3$ from the previously reported [13] 880–902 °C in this study may be due to the increase in the heating rate from 5 to 10 °C/min [11, 14]. Two endotherms were observed in the DTA curve, at 750 and 902 °C, consistent with the temperatures at which the downward sloping of TGA curves ended. A total of ~18.60% mass loss was recorded in the entire heating cycle from 30 to 1200 °C which is consistent (within ± 1%) with the total $CO_2$ forming during the reaction given in Eq. (3)

$$3SrCO_3{:}2CaCO_3{:}2Nb_2O_5{:}1TiO_2 \rightarrow Sr_3Ca_2Nb_4TiO_{17} + 5CO_2 \quad (3)$$

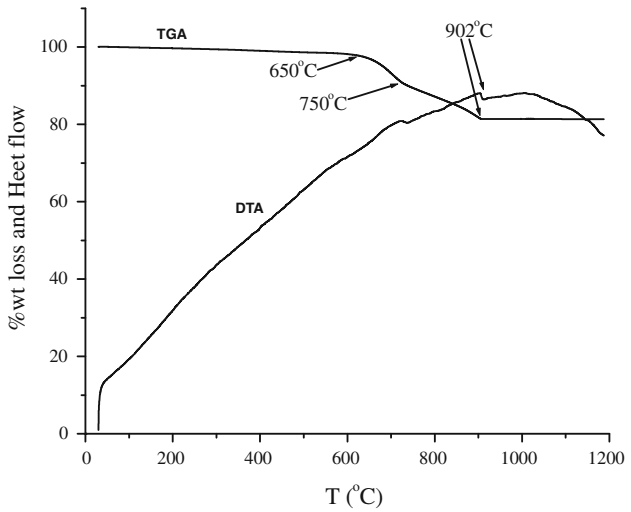


**Fig. 1** TG/DTA curves from the as mix-milled 3SrCO3:2CaCO3: 2Nb2O5:1TiO2 powders

## X-ray diffraction

The room-temperature XRD patterns recorded for the calcined and sintered (at 1450 and 1500 °C) $Sr_{5-x}Ca_xNb_4TiO_{17}$ ($x = 0$–5) samples are shown in Figs. 2 and 3. The major phase observed in the sample with $x = 0$ and calcined at 990 °C/2 h was $Sr_5Nb_4TiO_{17}$; however, a few XRD peaks matched JCPDS Card# 28–1247 for $Sr_2Nb_2O_7$ indicating incomplete reaction. XRD patterns from compositions with $x = 1$–4 calcined at 1350 °C/2 h were similar and matched JCPDS Card# 87–1170 for $Sr_5Nb_4TiO_{17}$ [10] indicating the formation of single-phase ceramics. It is noticeable that no JCPDS cards could be found for $Ca_5Nb_4TiO_{17}$ but the observed major XRD peaks for the composition with $x = 5$, matched JCPDS Card# 51–412 for $Ca_5Nb_5O_{17}$. Being isostructural with $Ca_5Nb_5O_{17}$, the peaks due to $Ca_5Nb_4TiO_{17}$ could be indexed according to a model analogous to the $Ca_5Nb_5O_{17}$ reported in JCPDS Card# 51–412. A few low intensity peaks matching the JCPDS Card# 47–1668 for orthorhombic $CaNbO_3$ and JCPDS Card# 39–1392 for $CaNb_2O_6$ were also observed which indicated second phase formation at $x = 5$.

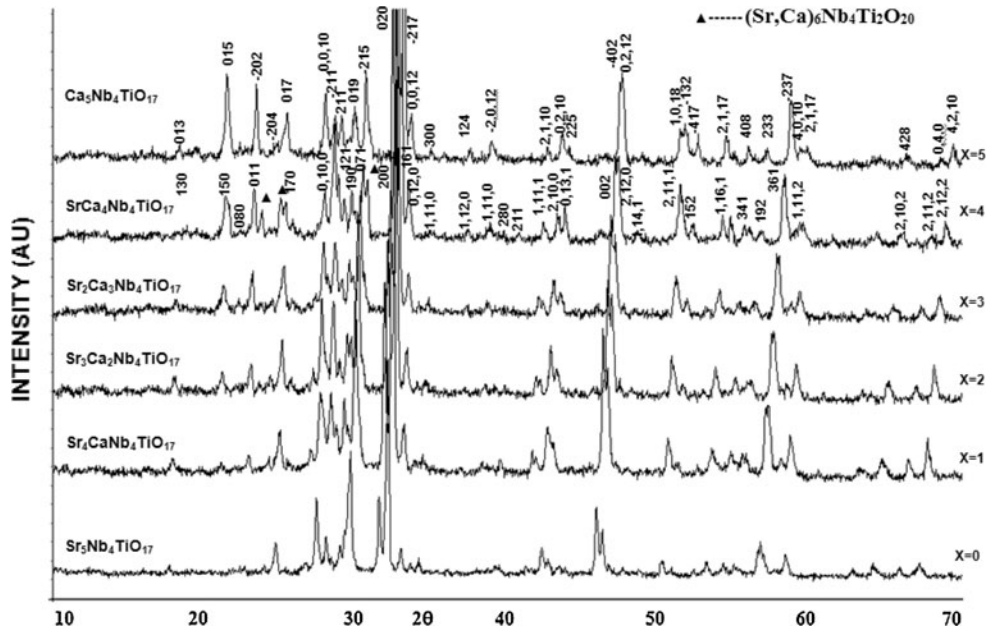


**Fig. 2** XRD patterns from $Sr_{5-x}Ca_xNb_4TiO_{17}$ samples with $x = 0$–5 sintered at 1450 °C for 2 h, showing the presence of single-phase compounds for $x = 0$, 1, 2, 3, and 5 and a mixture of layered perovskite $(Sr_{1-x}Ca_x)_n(Nb,Ti)_nO_{3n+2}$ phases with $n = 5$ and 6 for the $Sr_{5-x}Ca_xNb_4TiO_{17}$ composition with $x = 4$

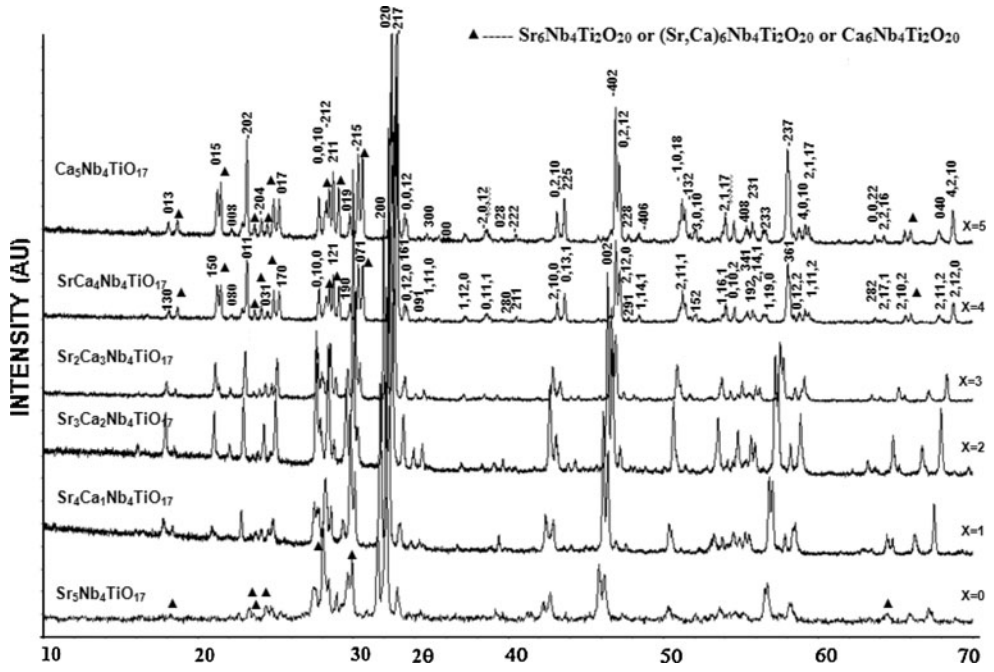


**Fig. 3** XRD patterns from $Sr_{5-x}Ca_xNb_4TiO_{17}$ samples with $x = 0$–5 sintered at 1500 °C for 2 h, showing the presence of a mixture of $(Sr_{1-x}Ca_x)_n(Nb,Ti)_nO_{3n+2}$ compounds with $n = 5$ and 6

The XRD of the samples sintered at 1450 °C for 2 h revealed the formation of single phases for the compositions with $x = 0$, 1, 2, 3, and 5, while a mixture of $n = 5$ and 6 layered perovskites was found for the composition with $x = 4$. No reference data cards could be found for the Ca versions of the compounds expected from the compositions with $x = 4$; however, these XRD peaks matched JCPDS Card# 87–1170 for $Sr_5Nb_4TiO_{17}$ and 49–544 for $Sr_6Nb_4Ti_2O_{20}$ with appropriate shifting of peak positions due to Ca substitution. Thus, $SrCa_4Nb_4TiO_{17}$ and $(Sr,Ca)_6Nb_4Ti_2O_{20}$, being isostructural with the compounds $Sr_5Nb_4TiO_{17}$ and $Sr_6Nb_4Ti_2O_{20}$, respectively, were indexed according to the models analogous to these compounds reported in JCPDS Card# 87–1170 and 49–544 (Fig. 2). Above 1450 °C, even the compositions with $x = 1$, 2, 3, and 5 were not single phase and XRD of samples sintered at 1500 °C for 2 h revealed the presence of a mixture of $(Sr_{1-x}Ca_x)_n(Nb,Ti)_nO_{3n+2}$ perovskite compounds with $n = 5$ and 6, i.e., $Sr_5Nb_4TiO_{17}$ (JCPDS Card# 87–1170) and $Sr_6Nb_4Ti_2O_{20}$ or $Ca_6Nb_4Ti_2O_{20}$ (JCPDS Card# 49–544) for $x = 0$ or 5, respectively. It is noticeable that at 1500 °C, the major phases observed in the compositions with $x = 1$, 2, 3, and 4 were $Sr_4CaNb_4TiO_{17}$, $Sr_3Ca_2Nb_4TiO_{17}$, $Sr_2Ca_3Nb_4TiO_{17}$, and $SrCa_4Nb_4TiO_{17}$, respectively; however, the nature of the secondary phases, i.e., the layered perovskites with $n = 6$ in compositions with $x = 1-4$, could not be identified. The crystal structure of the compounds with $x = 0-4$ was orthorhombic (*Pnnm*) and the compound with $x = 5$ crystallized into a monoclinic structure with space group $P2_1/b$ or

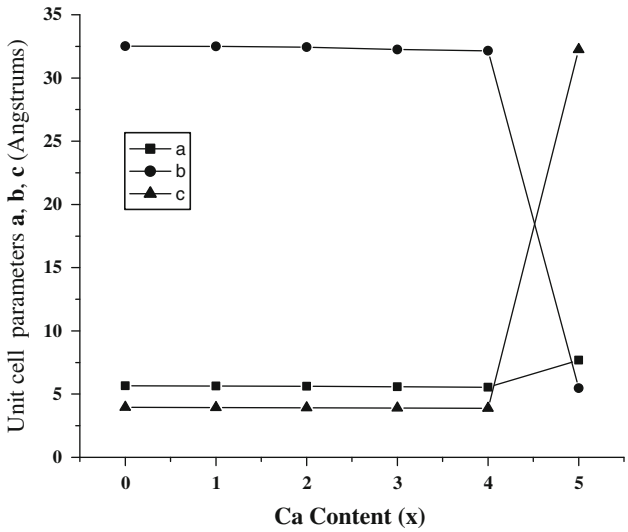


**Fig. 4** The variation of unit cell parameters with composition for the $Sr_{5-x}Ca_xNb_4TiO_{17}$ ceramics

$P2_1/c$ [8]. Manan et al. [13, 15] and Levin et al. [16] have also reported the formation of a mixture of $Sr_n(Nb,Ti)_nO_{3n+2}$ compounds with $n = 5$ and 6 in the $SrTiO_3$–$Sr_2Nb_2O_7$ system with no $Ca^{+2}$ substitution. The decomposition into secondary phases is more visible in the compositions with $x = 4$ and 5 as compared to the compositions with $x = 0-3$ sintered at 1500 °C/2 h (Fig. 3).

The compounds in the system $Sr_{5-x}Ca_xNb_4TiO_{17}$ crystallize into $A_5B_5O_{17}$ structure where the large Sr/Ca cations

**Table 1** Microwave dielectric properties of $Sr_{5-x}Ca_xNb_4TiO_{17}$ ($x = 0$–5)

| $x$ | $a$ (Å) | $b$ (Å) | $c$ (Å) | $\alpha$ (°) | $\beta$ (°) | $\gamma$ (°) | $z$ | $V$ (Å$^3$) | $V_m$ (Å$^3$) | Sintering Temp. (°C) | $\rho_{ap}$ (g/cm$^3$) | $\varepsilon_r$ | $Q_u \times f_o$ (GHz) | $\tau_f$ (ppm/°C) |
|---|---|---|---|---|---|---|---|---|---|---|---|---|---|---|
| 0 | 5.6614 | 32.515 | 3.9525 | 90 | 90 | 90 | 2 | 727.577 | 363.788 | 1500 | 4.46 | 48.9 | 447 | +162.4 |
| 1 | 5.6393 | 32.488 | 3.9365 | 90 | 90 | 90 | 2 | 721.21 | 360.605 | 1500 | 4.61 | 62.5 | 852 | −14.5 |
| 2 | 5.6193 | 32.444 | 3.9229 | 90 | 90 | 90 | 2 | 715.2 | 357.6 | 1500 | 4.74 | 61.8 | 1285 | +50.0 |
| 3 | 5.5754 | 32.252 | 3.8971 | 90 | 90 | 90 | 2 | 700.8 | 350.4 | 1500 | 4.57 | 53.4 | 1166 | –6.5 |
| 4 | 5.5360 | 32.151 | 3.8727 | 90 | 90 | 90 | 2 | 689.29 | 344.645 | 1500 | 4.39 | 42.2 | 1664 | –86.0 |
| 5 | 7.6889 | 5.4763 | 32.253 | 90 | 96° | 90 | 4 | 1358.06 | 339.515 | 1500 | 4.05 | 37.6 | 3087 | –132.5 |

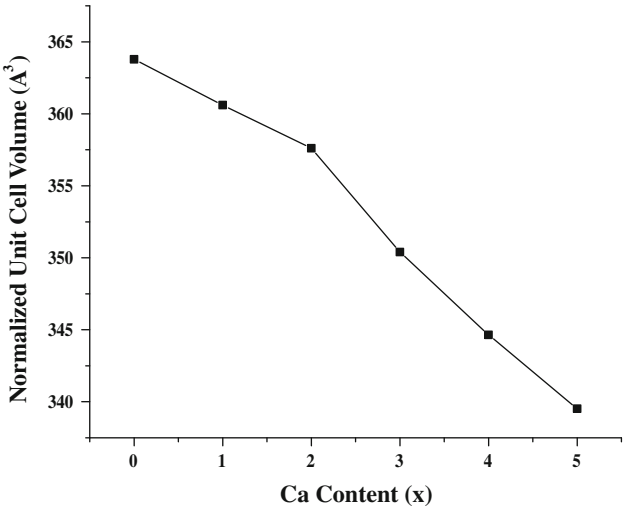


**Fig. 5** The plot of normalized unit-cell volume versus $x$ for $Sr_{5-x}Ca_xNb_4TiO_{17}$ ($x = 0$–5)

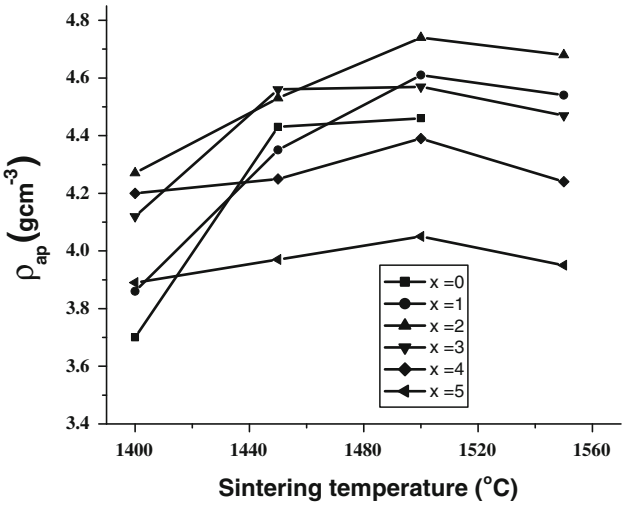


**Fig. 6** The variation in the apparent density of $Sr_{5-x}Ca_xNb_4TiO_{17}$ ($x = 0$–5) compounds with sintering temperature, showing the maximum density for the compound with $x = 2$

occupy the A site with coordination of 12 and the Ti/Nb cations occupy the B site with coordination of 6. The resulting structure consists of perovskite-like blocks each of which is five octahedra thick and separated by an extra layer of oxygen. With increasing $Ca^{+2}$ content from $x = 1$ to 5, the XRD peaks shifted toward higher diffraction angles, i.e., smaller interplanar spacings due to the smaller size of $Ca^{+2}$ (1.34 Å) substituted for the larger $Sr^{+2}$ (1.44 Å) ion [17, 18] resulting in a decrease in the lattice constants of the unit cell (Fig. 4).

The unit cell parameters of the $Sr_{5-x}Ca_xNb_4TiO_{17}$ ceramics refined by the least squares method are given in the Table 1. The lattice parameters '$a$', '$b$', and '$c$' decreased from 5.6614 to 5.5360 Å, 32.515 to 32.151 Å, and 3.9525 to 3.8727 Å, respectively, with increase in '$x$' from 0 to 4. For $x = 5$, '$a$' and '$c$' increased to 7.6889 and 32.253 Å, respectively, and '$b$' decreased to 5.4763 Å. This appears consistent with the observed change in structure from orthorhombic (*Pnnm*) [10] to monoclinic ($P2_1/c$) [19]. Consequently, the normalized cell volume ($V_m = V_{unit\ cell}/Z$) of the $Sr_{5-x}Ca_xNb_4TiO_{17}$ unit cell decreased from 363.788 ($x = 0$) to 339.515 Å$^3$ ($x = 5$) due to the substitution of the small $Ca^{+2}$ ion in the unit cell for the larger $Sr^{+2}$ ion as shown Fig. 5. The alternative orthorhombic arrangement can be obtained by reorienting the monoclinic unit cell with $a_m \parallel -a_o$, $b_m \parallel c_o$ and $c_m \parallel b_o$, where the subscripts 'm' and 'o' refer to the modified and original unit cell parameters.

## Density measurement

The variation in the apparent density of $Sr_{5-x}Ca_xNb_4TiO_{17}$ compounds ($x = 0$–5) with increase in sintering temperature is shown in Fig. 6. The density of each composition first increased with increase in the sintering temperature from 1400 to 1500 °C and then decreased with further increase in the sintering temperature to 1550 °C. This indicated that the density of each composition reached a maximum at ~1500 °C. A previous study [15] reported a maximum density of ~4.46 g/cm$^3$ for $Sr_5Nb_4TiO_{17}$ at ~1450 °C. In this study, a maximum density of ~4.74 g/cm$^3$ was achieved for the composition with

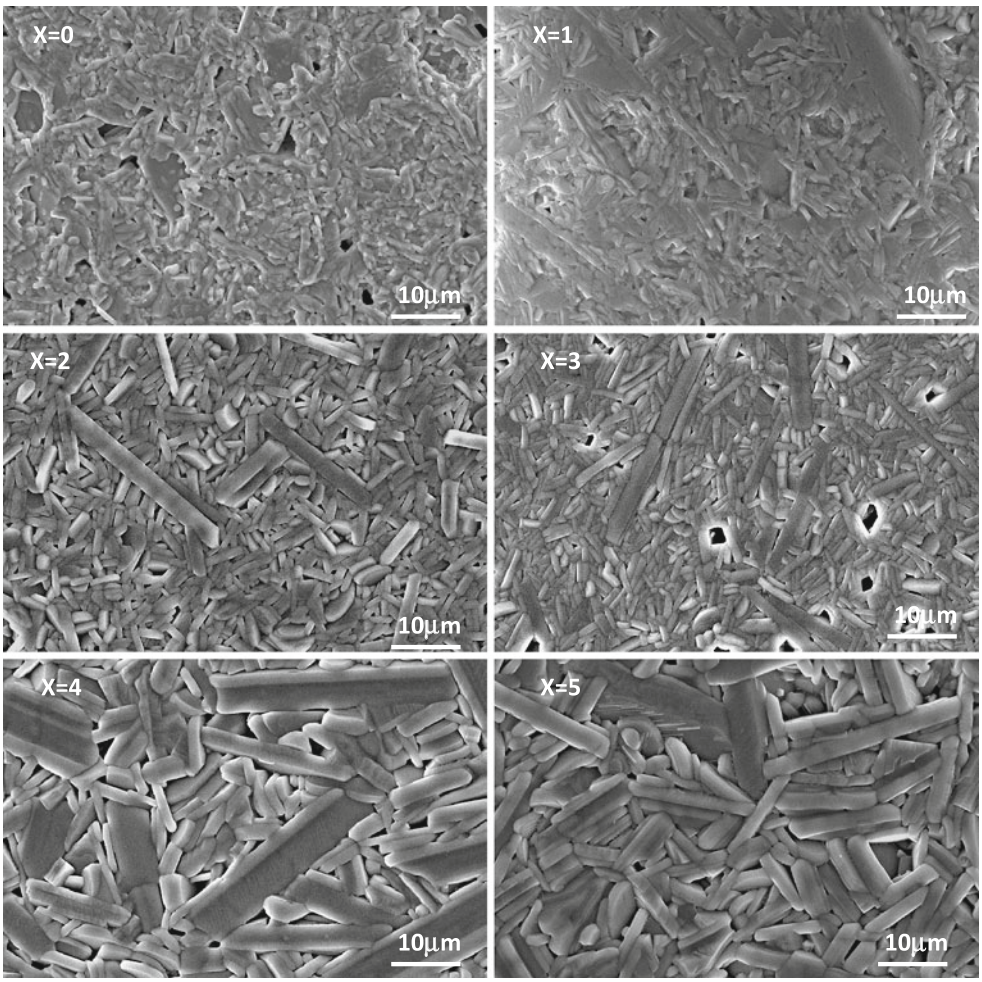


**Fig. 7** SEM images from thermally etched $Sr_{5-x}Ca_xNb_4TiO_{17}$ ($x = 0$–5) samples showing irregular grains for compositions with $x = 0$ and 1

$x = 2$, indicating an increase in the density due to the substitution of Ca for Sr.

## Microstructural analysis

The secondary electron images (SEI) from thermally etched $Sr_{5-x}Ca_xNb_4TiO_{17}$ ($x = 0$–5) samples sintered at ~1500 °C are shown in Fig. 7. The edges of the grains observed in sintered $Sr_{5-x}Ca_xNb_4TiO_{17}$ ceramics with $x = 0$ and 1 appeared less sharp in comparison to those with $x \geq 2$. As evident from Fig. 6, the density of these ceramics (with $x \leq 1$) was also observed to be lower than the other ceramics sintered at the same temperature, indicating the effect of calcium substitution upon sintering. In general, the grains were irregular in shape with varying size. The average grain size observed in the microstructure of the compositions with $x = 2$ and 3 was ~1 × 2–1.5 × 5 $\mu m^2$; however, a small number of elongated (~2.5 × 23 $\mu m^2$) grains were also observed. The number of elongated grains increased with increase in $x$ (i.e., $x = 4$, 5) consistent with the XRD results showing the splitting of the compound into layered $n = 5$ and 6 perovskites. The grains in the microstructure of the compositions with $x = 2$ and 3 appeared more compact than the other compositions, consistent with the observed higher density of these compounds in comparison to the others.

## Dielectric properties at low frequencies

In spite of forming multi-phasic ceramics, the dielectric properties of the compositions sintered at 1500 °C were better due to their relatively higher densities than those sintered at 1450 and 1550 °C. The variation in the dielectric constant ($\varepsilon_r$) and loss tangent ($\tan\delta$) with temperature measured at 1 kHz–1 MHz for $Sr_{5-x}Ca_xNb_4TiO_{17}$ (with $x = 0$–5) sintered at 1500 °C/2 h is shown in Figs. 8 and 9. Strong anomalies in $\varepsilon_r$ and $\tan\delta$ for the $x = 0$

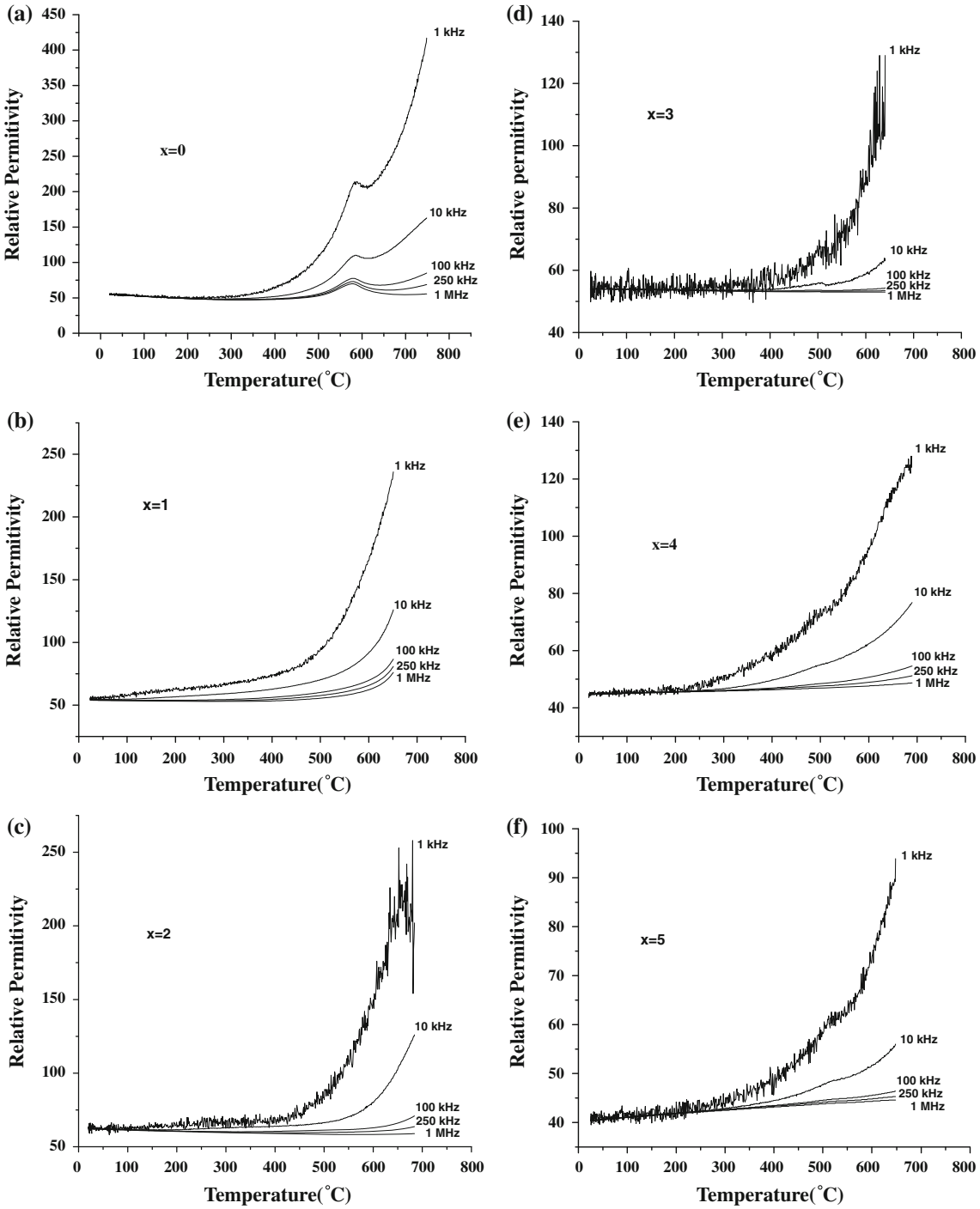


**Fig. 8** Variation of relative permittivity of $Sr_{5-x}Ca_xNb_4TiO_{17}$ ($x = 0$–5) with temperature at 1 kHz–1 MHz, showing anomalies at 531.3, 495.8, 492.5, and 514.9 °C for $x = 0$, 3, 4, and 5, respectively

compound, which may be due to the ferroelectric to para electric phase transition at ~531.3 °C, were observed. Similar behavior has been reported in $\varepsilon_r$ and tan$\delta$ measured for $Ba_{5-x}Sr_xDyTi_3V_7O_{30}$ (with $x = 0$–5) ceramics at 435, 355, 326, 82, and 46 °C [20]. The observed decrease in the dielectric constant with increase in frequency may be due to the vanishing of the contribution from interfacial and ionic polarization. Furthermore, a decrease in $\varepsilon_r$ was observed with increase in the Ca content due to the reduced ionic polarizability of $Ca^{+2}$ (3.17 Å$^3$) than the $Sr^{+2}$ (4.25 Å$^3$) [21]. The observed increase in tan$\delta$ with increase in temperature may be due to the increased conductivity of the compounds. [20]. The tan$\delta$ was observed to be the lowest for the composition with $x = 5$.

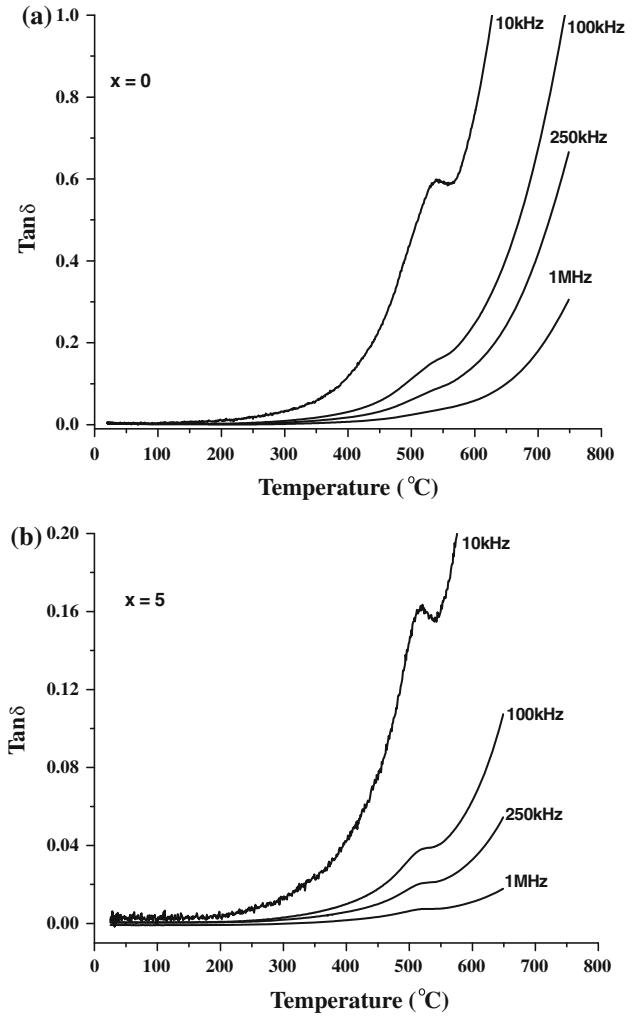


**Fig. 9** Variation of loss tangent for the $Sr_{5-x}Ca_xNb_4TiO_{17}$ compositions ($x = 0$ and 5) with temperature at 10 kHz–1 MHz showing low loss for the ceramics with $x = 5$

## Microwave dielectric properties

The microwave dielectric properties of the $Sr_{5-x}Ca_xNb_4TiO_{17}$ ($x = 0-5$) ceramics are given in Table 1. The unexpectedly low dielectric constant (48) observed for pure $Sr_5Nb_4TiO_{17}$ with no substitution may be due to its having the lowest density of all the compositions in this study. It is evident from Table 1 that the substitution of Ca decreased the dielectric constant and temperature coefficient of resonant frequency; however, the $Q_u \times f_o$ was not highly improved under the processing conditions employed in this study. The temperature coefficient of resonant frequency, $\tau_f$, for the composition with $x = 1$ was positive (+12.9 ppm/°C) when sintered at 1400 °C while negative (−2.5 and −14.5 ppm/°C) when sintered at 1450 and 1500 °C, respectively. The nature of the negative $\tau_f$ is not known. The substitution of Ca for Sr increased the $Q_u \times f_o$ value from 447 ($x = 0$) to 3087 GHz ($x = 5$), decreased the dielectric constant from 48 ($x = 0$) to 37.6 ($x = 5$). The substitution of Ca for Sr is known to cause tilting of octahedra [1] which may be the possible reason for the observed decrease in $\tau_f$ from 162.4 ppm/°C for $Sr_5Nb_4TiO_{17}$ to −132.5 ppm/°C for $Ca_5Nb_4TiO_{17}$.

## Conclusions

The effect of Ca substitution for Sr on the phase, microstructure and dielectric properties of $Sr_5Nb_4TiO_{17}$ was investigated. XRD revealed the formation of single-phase ceramics for the compositions with $x = 1$–4. Compositions with $x = 0$ and 5 showed the formation of secondary $Sr_2Nb_2O_7$ ($x = 0$), and $CaNbO_3$ and $CaNb_2O_6$ ($x = 5$) phases along with the parent $Sr_5Nb_4TiO_{17}$ and $Ca_5Nb_4TiO_{17}$ phases, respectively, upon calcination. XRD of the sintered samples with $x = 0$–5 showed the decomposition into $n = 5$ and 6 layered perovskites with the general formula $(Sr_{1-x}Ca_x)_n(Nb,Ti)_nO_{3n+2}$ at 1500 °C. Such decomposition was most evident in the compositions with $x = 4$ and 5. The layered perovskite with $n = 6$ in the compositions with $x = 0$ and 5 were $Sr_6Nb_4Ti_2O_{20}$ and $Ca_6Nb_4Ti_2O_{20}$, respectively; however, the nature of the layered perovskites with $n = 6$ in the compositions with $x = 1$–4 could not be identified. The normalized cell volume of the unit cell decreased with increase in the Ca content. The Ca substitution decreased the dielectric constant and $\tau_f$ and increased the $Q_u \times f_o$ (GHz) value.

**Acknowledgements** The authors acknowledge the financial support of the Higher Education Commission of Pakistan (NRPU 20-569, IRSIP and Development of Materials Connection Centre Pak-US Project ID 131) and the enormous support provided by Prof. I. M. Reaney and his group in facilitating the authors at the Electroceramics laboratory, Department of Engineering Materials, University of Sheffield (UK) and Dr. Rick Ubic, Boise State University (USA) for typographical corrections and guidance.

## References

1. Reaney IM, Idles D (2006) J Am Ceramic Soc 89(7):2068
2. Jawahar IN, Santha N, Sebastian MT, Mohanan P (2002) J Mater Res 17:3084
3. Zhao F, Yue Z, Gui Z, Li L (2006) J Am Ceram Soc 89(11):3421
4. Chen YC, Tsai JM (2008) J Appl Phys 47:7959
5. Chen YC, Yao SL, Jie R, Chen KC (2009) J alloys Compd 486:410
6. Anjana PS, Tony J, Sebastian MT (2007) IEEE electromagnetic conference, Kolkata, India
7. Tony J, Anjana PS, Letourneau S, Ubic R, Smaalen SV, Sebastian MT (2010) Matt Chem Phys 121(1–2):77
8. Slobodyanik NS, Titov YA, Chumak (2005) Theor Exp Chem 41(1):53
9. Iqbal Y, Reaney IM (2004) Ferroelectrics 302:259
10. Drews AR, Wong-Ng W, Roth RS, Vanderah TA (1996) Mat Res Bull 31(2):153

11. Sinton CW (2006) Raw materials for glass and ceramics sources, processes and quality control, John Willey & Son Inc, New York, p 151
12. Hungria T, Lisoni JG, Castro A (2002) Chem Mater 14:1747
13. Manan A, Iqbal Y, Qazi I (2008) J Pak Matt Soc 2(2):77
14. Zorel HE Jr, Guinesi LS, Ribeiro CA, Crespi MS (2000) Matt Lett 42:16
15. Manan A, Iqbal Y, Qazi I (2010) J Phys Conf Series 241:012028
16. Levin I, Leonid A, Bendersky A, Vanderah TA (2000) Phil Mag A 80(2):411
17. Pei J, Yue Z, Zhao F, Gui Z, Li L (2008) J Alloy Compd 459:390
18. Bijumon PV, Sebastian MT, Dias A, Moreira RL, Mohanan P (2005) J Appl Phys 97:104
19. Guevarra J, SchÖnleber A, Smaalen SV, Lichtenberg F (2007) Acta Cryst B 63:183
20. Sahoo PS, Panigrahi A, Patri SK, Choudhary RNP (2009) J Alloy Compd 484:832
21. Shannon RD (1993) J Appl Phys 73(1):348